Table 4. Analysis of variance results of the case–institution model (a) and of the case–method model (b)

	PTVmax	PTVmin	D95	HI	CI
(a) Sum of squares					
Model	14.0	445	260	0.410	3.24
Case	1.0 (P = 0.538)	27 (P = 0.205)	16 (P = 0.564)	0.038 (P = 0.134)	0.74 (P = 0.149)
Institution	13.0 (P = 0.015*)	418 (P<0.001*)	244 (P = 0.007*)	0.372 (P<0.001*)	2.50 (P = 0.081)
Error	14.1	166	229	0.192	3.89
R^2	0.499	0.728	0.532	0.681	0.454
(b) Sum of squares					
Model	12.0	451	302	0.421	2.82
Case	1.3 (p = 0.480)	33 (p = 0.117)	4 (p = 0.876)	0.043 (p = 0.080)	0.82 (p = 0.141)
Calculation algorithm	4.9 (p = 0.039*)	96 (p = 0.002*)	117 (p = 0.002*)	0.070 (p = 0.016*)	1.05 (p = 0.077)
Beam energy	2.8 (p = 0.166)	31 (p = 0.132)	42 (p = 0.097)	0.016 (p = 0.446)	0.38 (p = 0.449)
Irradiation technique	1.0 (p = 0.577)	52 (p = 0.032*)	22 (p = 0.323)	0.071 (p = 0.015*)	0.50 (p = 0.326)
Error	16.1	160	188	0.181	4.32
R^2	0.428	0.738	0.617	0.700	0.395

Abbreviation: PTV = planning target volume; HI = homogeneity index; CI = conformity index.

The degrees of freedom were three in case, ten in institution, three in calculation algorithm, three in beam energy, and three in irradiation technique.

The intercase variations were not significant for any of the PTV data. The interinstitutional variations were significant for PTVmax, PTVmin, D95, and HI. The R^2 of the case-method model were similar to those of the case-institution model. In the case-method model, the calculation algorithm was significant for PTVmax, PTVmin, D95, and HI and the irradiation technique was significant for PTVmin and HI.

* Asterisks (*) indicate the statistical significance of the factors.

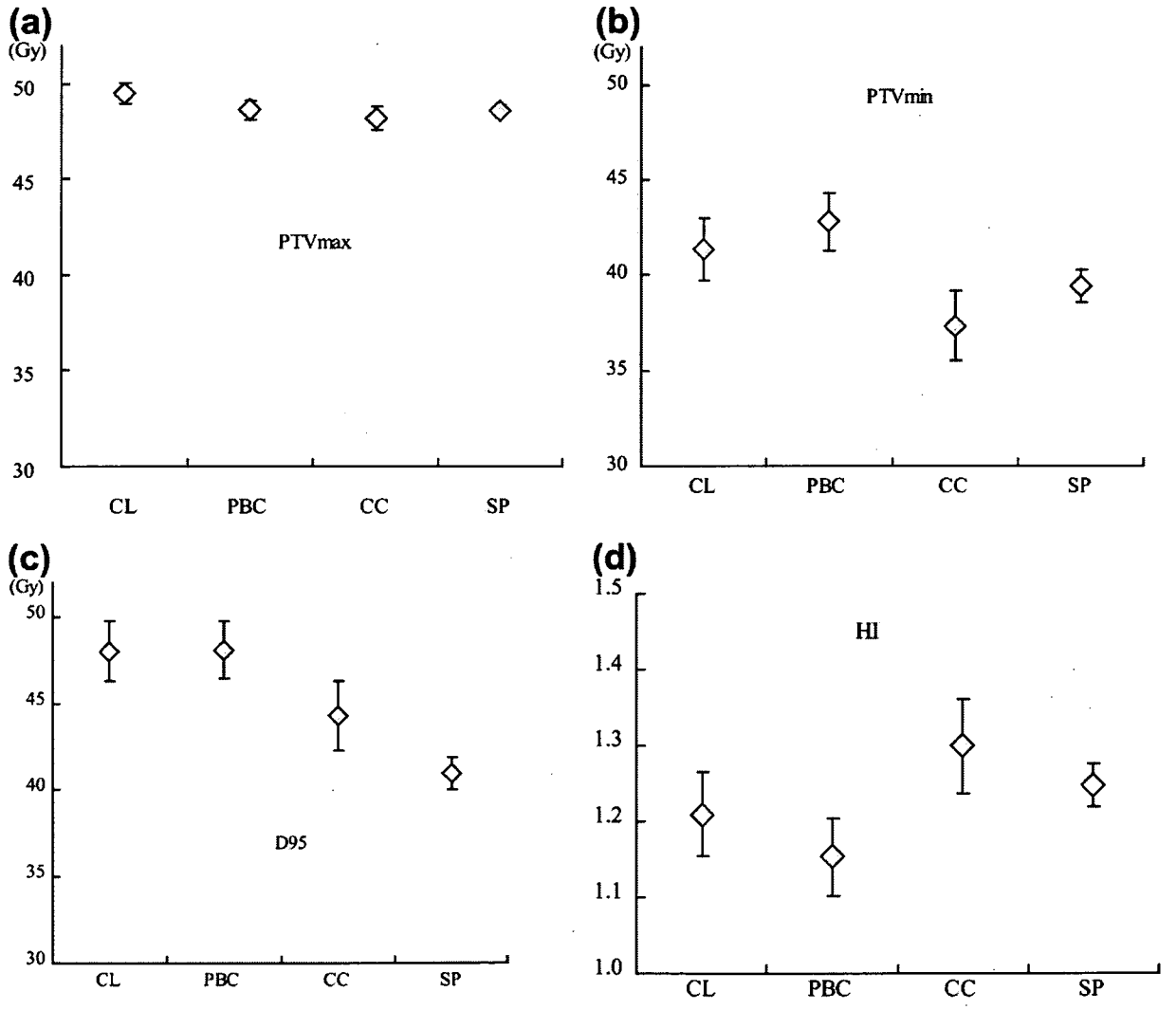

Fig. 3. Dose–volumetric data of planning target volume (PTV) grouped by calculation algorithms; (a) PTVmax, (b) PTVmin, (c) D95, and (d) homogeneity index (HI). Diamonds and bars indicate means and standard errors, respectively. The PTVmax was significantly lower with collapsed cone convolution super position (CC) than with effective path length correction (CL) (p = 0.038). The PTVmin was significantly lower with CC than with CL (p = 0.047) and Batho power law correction (PBC) (p = 0.001). The D95 was significantly lower with superposition (SP) than with CL (p = 0.010) and PBC (p = 0.004). The HI was significantly higher with CC than with PBC (p = 0.012).

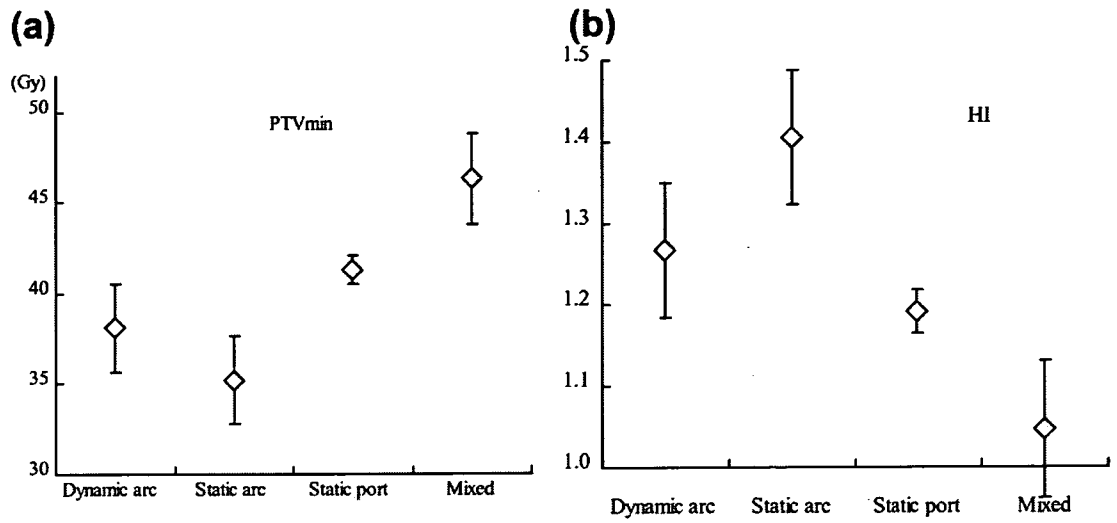

Fig. 4. Dose–volumetric data of planning target volume (PTV) grouped by irradiation method; (a) PTVmin and (b) homogeneity index (HI). Diamonds and bars indicate means and standard errors, respectively. The static-arc method is significantly lower for PTVmin ($p = 0.023$) and significantly higher for HI ($p = 0.017$) than the static-port method.

for the spinal cord and the lung. The PRV for the spinal cord was defined as a 3-mm margin with the spinal canal delineated on CT images. The PRV for the lung was defined as the bilateral pulmonary parenchyma outside the PTV. The prescription dose was 48 Gy in 12-Gy fractions at the isocenter. Beam energy, arrangement of irradiation ports, and dose calculationculation were identical to those used clinically at each institution. Created plans should satisfy the dose constraints for the protocol.

Evaluated data

The participating institutions submitted the following data as their planning results: volume of the GTV or ITV; maximal dose (PTVmax), minimal dose (PTVmin), D95 (dose covering 95% volume of PTV), homogeneity index (HI; equal to the maximal dose divided by the minimal dose) and conformity index (CI; equal to the treated volume, which we defined as the volume enclosed by the isodose curve of the PTVmin, divided by PTV volume) of the PTV; mean dose, 40-Gy irradiated volume, V15 (percentage of volume covered by 15-Gy isodose line) and V20 (percentage of volume covered by 20-Gy isodose line) of the PRV for the lung; maximal dose of the PRV for the spinal cord; and 48-Gy– and 40-Gy–irradiated volumes of the PRV for the heart in Case 2 and those of the PRV for the aorta in Case 3. The volumes of GTV and ITV were evaluated as indices of target delineation, and the other dose–volumetric data were evaluated as indices of dose distributions.

Statistical analysis

To assess the significance of the interinstitutional variations, analysis of variance (ANOVA) was performed for a fixed-effect model with the two independent factors of case and institution (case–institution model). All pairwise comparisons were performed using Tukey's Studentized range test, and ANOVA was performed for another fixed effect model with the factors of case, calculation algorithm, beam energy, and irradiation technique (case–method model) to investigate the main cause of the interinstitutional variations. The validity of the case–method model was assessed with comparison of R^2 with that of the case–institution model.

Variations in the target volumes of each case were evaluated

Table 5. Variations in doses to organs at risk (OAR)

PRV	Case 1	Case 2	Case 3	Case 4
Lung				
Mean dose (Gy)	2.5 (2.1–3.3)	5.5 (4.3–7.7)	2.8 (2.0–3.9)	6.9 (6.0–9.0)
40-Gy irradiated volume (cc)	21.8 (1.0–45.1)	39.6 (18.0–79.0)	26.2 (8.0–56.6)	67.0 (39.0–99.6)
V15 (%)	3.9 (2.3–6.0)	12.1 (9.0–17.8)	4.1 (2.5–6.1)	17.2 (14.2–24.0)
V20 (%)	2.5 (1.6–4.0)	7.8 (5.0–12.4)	2.7 (1.8–4.1)	11.8 (8.3–19.0)
Spinal cord				
Maximal dose (Gy)	4.6 (0.2–13.3)	8.8 (2.7–16.9)	7.2 (0.6–14.2)	9.7 (2.3–18.4)
Heart				
48-Gy irradiated volume (cc)		0.0 (0.0–0.0)		
40-Gy irradiated volume (cc)		1.0 (0.0–5.5)		
Aorta				
48-Gy irradiated volume (cc)			0.0 (0.0–0.0)	
40-Gy irradiated volume (cc)			1.0 (0.0–5.3)	

Abbreviation: PRV = planning OAR volume.
Data are shown as mean (range).

with the coefficient of variation (CV), which is equal to the standard deviation (SD) divided by the mean. The overall CV in the study was defined as the mean SD divided by the overall mean of all cases.

RESULTS

Table 1 summarizes the characteristics of the participating institutions. Six institutions performed treatment planning with FOCUS/XiO (CMS, St. Louis, MO), three with Eclipse (Varian, Palo Alto, CA), one with Cadplan (Varian), and one with Pinnacle3 (Philips/ADAC, Milpitas, CA). Dose calculation algorithms of Clarkson with effective path length correction (CL) and superposition (SP) were used in FOCUS/XiO; pencil beam convolution with Batho power law correction (PBC) was used in Eclipse and Cadplan; and collapsed cone convolution superposition (CC) was used in Pinnacle3. Institutions E and F used the algorithm CL in the first series and used SP in the second series. Most institutions used 6-MV x-rays except for institutions B (10 MV), H (6 and 10 MV), and J (4 MV). Institution B used a mixed style of dynamic arcs and static ports in the first series and then used multiple static ports in the second series. Institution D used the multiple static arc technique with fixed rectangular ports, and institution E used the multiple dynamic conformal arc technique. The remaining eight institutions created multiple static port plans.

Variations in the target volumes

Target volumes measured by the 11 institutions in the four cases are shown in Table 2. The CVs were 17.9%, 16.8%, 32.7%, and 11.2% in Cases 1, 2, 3, and 4, respectively. The overall CV was 16.6%. Analysis of variance (ANOVA) of the target volumes in the case–institution model showed that the interinstitutional variations were not significant ($p = 0.089$).

Variations in the dose–volumetric data

The dose–volumetric data of the PTVs are shown in Table 3 and Figure 2. The ANOVA in the case–institution model (Table 4a) showed that the intercase variations were not significant. On the other hand, the interinstitutional variations were significant for PTVmax ($p = 0.014$), PTVmin ($p < 0.001$), D95 ($p = 0.007$), and HI ($p < 0.001$). The maximal differences in mean levels of institution were 2.1 Gy for PTVmax (between institutions E and K), 10.2 Gy for PTVmin (between institutions C and D), 7.8 Gy for D95 (between institutions D and K), and 0.33 for HI (between institutions D and I). For PTVmax, PTVmin, D95, and HI, the R^2 of the case–method models were similar to those of the case–institution models (Table 4b). The ANOVA of the case–method model showed that the dose calculation algorithm was significant for PTVmax ($p = 0.039$), PTVmin ($p = 0.002$), D95 ($p = 0.002$), and HI ($p = 0.016$) and that the irradiation technique was significant for PTVmin ($p = 0.032$) and HI ($p = 0.015$). Comparison of the calculation algorithms (Fig. 3) showed that the PTVmax was significantly lower with CC than with CL ($p = 0.038$). The PTVmin was significantly lower with CC than with CL ($p = 0.047$) and PBC ($p = 0.001$). The D95 was significantly lower with SP than with CL ($p = 0.010$) and PBC ($p = 0.004$). The HI was significantly higher with CC than with PBC ($p = 0.012$). With regard to the irradiation technique (Fig. 4), the differences between the static-arc method and the static-port method were significant for PTVmin ($p = 0.023$) and for HI ($p = 0.017$).

In the OARs, no violation of the dose constraints for the protocol was observed (Table 5).

DISCUSSION

Use of SBRT enables high-dose areas limited to target volume and reduces doses delivered to other areas. Therefore, SBRT planning depends greatly on target delineation. Variations in target delineation of lung cancer have been reported by several investigators (13–15). Bowden *et al.* reported that interclinician variations in measured volumes of lung tumor GTV ranged from 5.0% to 38.6% (mean, 20%) in CV in the first series of their study (13). In a study by Senan *et al.*,the interobserver variations in GTV were 0.60 cc, 4.80 cc, and 12.86 cc in SD for three lung tumors with mean volumes of 4.7 cc, 20.3 cc, and 88.6 cc, respectively (14), and the calculated mean CV in the study was 17.0%. Sakamoto *et al.* reported the mean CV in ITV volumes of 17.6% (15).

Our finding that the overall CV was 16.6% was consistent with these reports and raises questions about whether there should be concern about this level of variation, especially for small lesions. The CV in Case 3, for example, was the largest in this study; there was a difference of more than threefold between the maximum and minimum ITV estimates. The large CV in this case might be caused by the motion blur being relatively large compared with the tumor size, and by small vessels or spiculations being observed around the tumor. It is important to make efforts to reduce the variations in target delineation. In the Bowden *et al.* study, the mean CV decreased to 13% in their second series after a 3-year interval from the first series. They repeated the exercise using a protocol derived from the experience of the first series. Their protocol included contouring issues on slice thickness and window settings of CT images and handling of such CT findings as spiculations, cavitations, and ateclectasis. Although slice thickness (3 mm or less) and window settings for delineation (level −700; width 2,000) were defined in our study, whereas handling of spiculations was not defined; that fact might result in the large CV in Case 3. In the JCOG 0403 protocol, the first case of each institution was reviewed by all participating institutions, and all cases will be reviewed by the study coordinator.

Before this study, the physics group of JCOG 0403 performed a phantom study in all institutions to ensure the accuracy of isocenter dose calculated with the treatment planning systems by a comparison of the measured dose using a phantom specially made for lung SBRT (16). The median differences between calculation and measurement

ranged from 0% to −1% for superposition/convolution algorithms and from 3% to 4% for the other older algorithms. The standard deviations between institutions were the same (2%) for the two groups of algorithms. Thus, it was thought that the calculation accuracy was assured for the isocenter dose in the participating institutions.

The dose distribution of the radiation plan generally depends on multiple factors such as target volume, beam energy, irradiation technique, and calculation algorithm. In this study, the interinstitutional variations were significant in the dose–volumetric data of the PTV. Comparison of the R^2 of the case–method model with those of the case–institution model suggested that the method factors (calculation algorithm, beam energy, and irradiation technique) could account for these interinstitutional variations. Among the method factors, the dose calculationculation algorithm was considered to be the most significant factor.

Task Group No. 65 of the Radiation Therapy Committee of the American Association of Physicists in Medicine categorized inhomogeneity correction algorithms according to the level of anatomy sampled for scatter calculation and the inclusion or exclusion of electron transport (17). The effective path length (EPL) correction performs a ray-trace from the source to the calculation point and scales the depth with the radiologic density along that ray. The EPL correction applies only to primary photons, and lateral electron transports and distribution of scattered photons are ignored (18). The Batho power law (BPL), as well as the EPL, is classified into a simplistic one-dimensional equivalent path correction without consideration of electron transport. The SP and CC are superposition/convolution algorithms that consider three-dimensional scatter calculations with electron transport (19, 20). It is generally accepted that dose distributions with superposition/convolution algorithms are more accurate than those with older inhomogeneity correction algorithms (21–23). The task group recommends that the superposition/convolution algorithm be considered for ascertaining dosage at tumor/lung interfaces in radiation planning for the lung, and that simplistic one-dimensional equivalent path corrections are reasonable only for point dose estimations for lung tumors. In the JCOG 0403 protocol, the dose prescription is defined as a point dose at the isocenter. Most of our clinical experiences, which are the basis for the JCOG 0403, involved the older algorithms, such as the BPL and the EPL. Superposition/convolution algorithms were not available in some institutions (*e.g.*, Eclipse/Cadplan users) at the time when we started the trial. Thus we have agreed that we would not use the superposition/convolution algorithms for the JCOG 0403 protocol to maintain continuing with our treatment experiences and to avoid algorithm-induced interinstitutional variations. We have a plan to use peripheral-dose prescription with superposition/convolution algorithms for an upcoming SBRT study of JCOG. Dose–volumetric data of cases registered for the present trial (JCOG 0403) are recalculated with the superposition/convolution algorithms, if available. These data are collected for the upcoming SBRT study and for a comparison with other studies.

Deviations of institution D in the dose–volumetric data of PTV were marked. The reasons for the marked deviations were thought to be use of the multiple–static-arc technique without a multileaf collimator and use of the SP algorithm. After the study, institution D changed its irradiation technique to multiple static ports and changed the algorithm from SP to CL.

This study was a kind of pretrial "dry run" or dummy run. Dummy runs play an important role in quality assurance (QA) for radiotherapy in clinical trials (24). Through this study, we shared our thoughts concerning treatment planning with other participants and recognized the interinstitutional variations. The importance of QA programs was recognized. The Advanced Technology Consortium (ATC) supports QA of the JCOG 0403. The CT images, structure sets, treatment plans, and dose distributions of all registered cases are sent to the ATC. With the remote review tool provided by the ATC, all plans can be reviewed and their quality can be confirmed.

In conclusion, there can be notable interinstitutional variations in planning for SBRT, including interobserver variations in estimates of target volumes as well as dose calculation effects related to the use of different dose calculation algorithm.

REFERENCES

1. Uematsu M, Shioda A, Suda A, *et al.* Computed tomography-guided frameless stereotactic radiotherapy for stage I non-small cell lung cancer: A 5-year experience. *Int J Radiat Oncol Biol Phys* 2001;51:666–670.
2. Nagata Y, Negoro Y, Aoki T, *et al.* Clinical outcomes of 3D conformal hypofractionated single high-dose radiotherapy for one or two lung tumors using a stereotactic body frame. *Int J Radiat Oncol Biol Phys* 2002;52:1041–1046.
3. Fukumoto S, Shirato H, Shimzu S, *et al.* Small-volume image-guided radiotherapy using hypofractionated, coplanar, and noncoplanar multiple fields for patients with inoperable Stage I nonsmall cell lung carcinomas. *Cancer* 2002;95:1546–1553.
4. Onimaru R, Shirato H, Shimizu S, *et al.* Tolerance of organs at risk in small-volume, hypofractionated, image-guided radiotherapy for primary and metastatic lung cancers. *Int J Radiat Oncol Biol Phys* 2003;56:126–135.
5. Timmerman R, Papiez L, McGarry R, *et al.* Extracranial stereotactic radioablation: Results of a phase I study in medically inoperable stage I non-small cell lung cancer. *Chest* 2003;124:1946–1955.
6. Onishi H, Araki T, Shirato H, *et al.* Stereotactic hypofractionated high-dose irradiation for stage I nonsmall cell lung carcinoma: Clinical outcomes in 245 subjects in a Japanese multiinstitutional study. *Cancer* 2004;101:1623–1631.
7. Onishi H, Kuriyama K, Komiyama T, *et al.* Clinical outcomes of stereotactic radiotherapy for stage I non-small cell lung cancer using a novel irradiation technique: Patient self-controlled breath-hold and beam switching using a combination of linear accelerator and CT scanner. *Lung Cancer* 2004;45:45–55.
8. Hof H, Herfarth KK, Munter M, *et al.* Stereotactic single-dose radiotherapy of stage I non-small-cell lung cancer (NSCLC). *Int J Radiat Oncol Biol Phys* 2003;56:335–341.

9. Wulf J, Haedinger U, Oppitz U, *et al.* Stereotactic radiotherapy for primary lung cancer and pulmonary metastases: A noninvasive treatment approach in medically inoperable patients. *Int J Radiat Oncol Biol Phys* 2004;60:186–196.
10. Zimmermann FB, Geinitz H, Schill S, *et al.* Stereotactic hypofractionated radiation therapy for stage I non-small cell lung cancer. *Lung Cancer* 2005;48:107–114.
11. Nagata Y, Takayama K, Matsuo Y, *et al.* Clinical outcomes of a phase I/II study of 48 Gy of stereotactic body radiotherapy in 4 fractions for primary lung cancer using a stereotactic body frame. *Int J Radiat Oncol Biol Phys* 2005;63:1427–1431.
12. Takeda A, Kunieda E, Shigematsu N, *et al.* Small lung tumors: Long-scan-time CT for planning of hypofractionated stereotactic radiation therapy—initial findings. *Radiology* 2005;237: 295–300.
13. Bowden P, Fisher R, Mac Manus M, *et al.* Measurement of lung tumor volumes using three-dimensional computer planning software. *Int J Radiat Oncol Biol Phys* 2002;53:566–573.
14. Senan S, van Sornsen de Koste J, Samson M, *et al.* Evaluation of a target contouring protocol for 3D conformal radiotherapy in non-small cell lung cancer. *Radiother Oncol* 1999;53:247–255.
15. Sakamoto M, Nagata Y, Takayama K, *et al.* Inter-observer variation in target delineation of stage I lung cancer for stereotactic radiotherapy *Int J Radiat Oncol Biol Phys* 2005;63: S411–S412.
16. Nishio T, Kunieda E, Shirato H, *et al.* Dosimetric verification in participating institutions in a stereotactic body radiotherapy trial for stage I non-small cell lung cancer: Japan Clinical Oncology Group trial (JCOG0403) *Phys Med Biol* 2006;51:5409–5417.
17. Task Group No. 65 of the Radiation Therapy Committee of the American Association of Physicists in Medicine. Tissue inhomogeneity corrections for megavoltage photon beams. Madison, WI: Medical Physics Publishing; 2004.
18. Chetty IJ, Rosu M, McShan DL, *et al.* The influence of beam model differences in the comparison of dose calculation algorithms for lung cancer treatment planning. *Phys Med Biol* 2005;50:801–815.
19. Miften M, Wiesmeyer M, Monthofer S, *et al.* Implementation of FFT convolution and multigrid superposition models in the FOCUS RTP system. *Phys Med Biol* 2000;45:817–833.
20. Ahnesjo A. Collapsed cone convolution of radiant energy for photon dose calculationculation in heterogeneous media. *Med Phys* 1989;16:577–592.
21. De Jaeger K, Hoogeman MS, Engelsman M, *et al.* Incorporating an improved dose calculationculation algorithm in conformal radiotherapy of lung cancer: Re-evaluation of dose in normal lung tissue. *Radiother Oncol* 2003;69:1–10.
22. Haedinger U, Krieger T, Flentje M, *et al.* Influence of calculation model on dose distribution in stereotactic radiotherapy for pulmonary targets. *Int J Radiat Oncol Biol Phys* 2005;61: 239–249.
23. Arnfield MR, Siantar CH, Siebers J, *et al.* The impact of electron transport on the accuracy of computed dose. *Med Phys* 2000;27:1266–1274.
24. Ottevanger PB, Therasse P, van de Velde C, *et al.* Quality assurance in clinical trials. *Crit Rev Oncol Hematol* 2003;47: 213–235.

APPENDIX: SUMMARY OF THE JAPAN CLINICAL ONCOLOGY GROUP (JCOG) 0403 PROTOCOL

TARGET VOLUME DEFINITION

Gross tumor volume (GTV)

The GTV is defined as gross disease determined from imaging modalities. GTV should generally be delineated using the CT pulmonary window (level −700; width 2,000).

Clinical target volume (CTV)

The CTV is identical to GTV in this trial.

Internal target volume (ITV)

The ITV consists of CTV and an internal margin that compensates for internal organ motions. Using long scan-time CT, ITV can be directly delineated on the images.

Planning target volume (PTV)

The PTV consists of ITV and a setup margin. The setup margin is 5 mm.

ORGAN-AT-RISK VOLUME DEFINITION

Planning organ-at-risk volume (PRV)

The PRVs are defined for lung, spinal cord, esophagus, stomach, intestine, trachea, bronchus, and other organs at risk (OARs). The margin between PRV and OAR is 5 mm, except for the spinal cord and the lung. The PRV for the spinal cord is defined as a 3-mm margin with the spinal canal delineated on CT images. The PRV for the lung is the bilateral pulmonary parenchyma outside the PTV.

Dose prescription and calculation

The prescribed dose is 48 Gy in 4 fractions at the isocenter. Noncoplanar static beams (5–10 ports) or multiple-arc beams (total 400 degrees or more) with 4- to 10-MV x-rays are allowed. The margin between the PTV and the field edge is about 5 mm. The dose distribution must be calculated with calculation matrices 2.5 mm or smaller and with inhomogeneity correction enabled.

Dose constraints

The HI of PTV must not exceed 1.6. The dose constraints for the OARs are shown in Table 6.

Table 6. Dose constraints of organs at risk (OARs) for the Japan Clinical Oncology Trial 0403 protocol (as of June 2004)

PRV	Constraint
Lung	Mean dose ≤ 18 Gy
	40-Gy irradiated volume ≤ 100 cc
	V15 ≤ 25%
	V20 ≤ 20%
Spinal cord	Maximal dose ≤ 25 Gy
Esophagus	40-Gy irradiated volume ≤ 1 cc
	35-Gy irradiated volume ≤ 10 cc
Stomach and intestine	36-Gy irradiated volume ≤ 10 cc
	40-Gy irradiated volume ≤ 100 cc
Trachea and main bronchi	40-Gy irradiated volume ≤ 10 cc
Other organs	48-Gy irradiated volume ≤ 1 cc
	40-Gy irradiated volume ≤ 10 cc

Abbreviation: PRV = planning OAR volume.

Int J Clin Oncol (2007) 12:3–7
DOI 10.1007/s10147-006-0646-6

REVIEW ARTICLE

Yasushi Nagata · Yukinori Matsuo · Kenji Takayama
Yoshiki Norihisa · Takashi Mizowaki
Michihide Mitsumori · Keiko Shibuya · Shinsuke Yano
Yuichiroh Narita · Masahiro Hiraoka

Current status of stereotactic body radiotherapy for lung cancer

Received: December 5, 2006

Abstract Stereotactic radiotherapy (SRT) for extracranial tumors has been recently performed to treat lung and liver cancers, and has subsequently been named stereotactic body radiotherapy (SBRT). The advantages of hypofractionated radiotherapy for treating lung tumors are a shortened treatment course that requires fewer trips to the clinic than a conventional program, and the adoption of a smaller irradiated volume allowed by greater setup precision. This treatment is possible because the lung and liver are considered parallel organs at risk. The preliminary clinical results, mostly reported on lung cancer, have been very promising, including a local control rate of more than 90%, and a relatively low complication rate. The final results of a few clinical trials are awaited. SBRT may be useful for the treatment of stage I lung tumors.

Key words Stereotactic body radiotherapy · Conformal radiotherapy · Lung cancer · Stereotactic body frame · Stereotactic radiotherapy · Extracranial tumors

Introduction

Stereotactic radiotherapy (SRT) for extracranial tumors has been recently performed to treat extracranial tumors, mainly lung and liver cancers, and has subsequently been named stereotactic body radiotherapy (SBRT) or extracranial stereotactic radiotherapy (ESRT). The advantages of hypofractionated radiotherapy for treating lung tumors are a shortened treatment course that requires fewer trips to the clinic than a conventional program, and the adoption of a smaller irradiated volume allowed by greater setup precision. This treatment is possible because the lung and liver are considered parallel organs at risk (OAR). The disadvantages of SBRT are the uncertain effects of altered fractionation and the theoretical risk of worsening the ratio of normal tissue to tumor tissue through the use of a high dose per fraction. In this article, the technical procedures and clinical results of SBRT, especially in lung cancer, are reviewed.

Y. Nagata (✉) · Y. Matsuo · K. Takayama · Y. Norihisa · T. Mizowaki · M. Mitsumori · K. Shibuya · S. Yano · Y. Narita · M. Hiraoka
Department of Therapeutic Radiology and Oncology, Kyoto University, Graduate School of Medicine, Sakyo, Kyoto 606-8507, Japan
Tel. +81-75-751-3762; Fax +81-75-751-3418
e-mail: nag@kuhp.kyoto-u.ac.jp

Biology

The biological background of SBRT is important. There is no past clinical evidence for this kind of hypofractionated regimen to extracranial tumors; therefore, most clinical regimens should be based on biological estimations.

The two great issues in hypofractionated regimens are dose response for tumor control and toxicity to normal tissue. Can the conventional linear-quadratic (LQ) model be applied in the SBRT dose range? Can repopulation be avoided in the SBRT regimen? How great is the effect of hypoxia in SBRT?

Fowler et al.[1] answered these questions, which are mostly applicable to SBRT; however, they recommended that SBRT be performed three to five fractionated schedule rather than using single SRS. These biological speculations should be reconfirmed in the clinical setting.

Body fixation

The first body fixation device was introduced in clinical practice as a stereotactic body frame by Bromgren et al.[2] and Lax et al.[3] Patients were fixed in the stereotactic frame, using a vacuum pillow. The concept of this frame is to utilize the cranial SRT coordinates for extracranial SBRT. The difference between cranial SRT and extracranial SBRT is the accuracy of the setup. The Japanese national guidelines for SRT state that the allowance of setup error is 2 mm for cranial tumors and 5 mm for extracranial tumors.

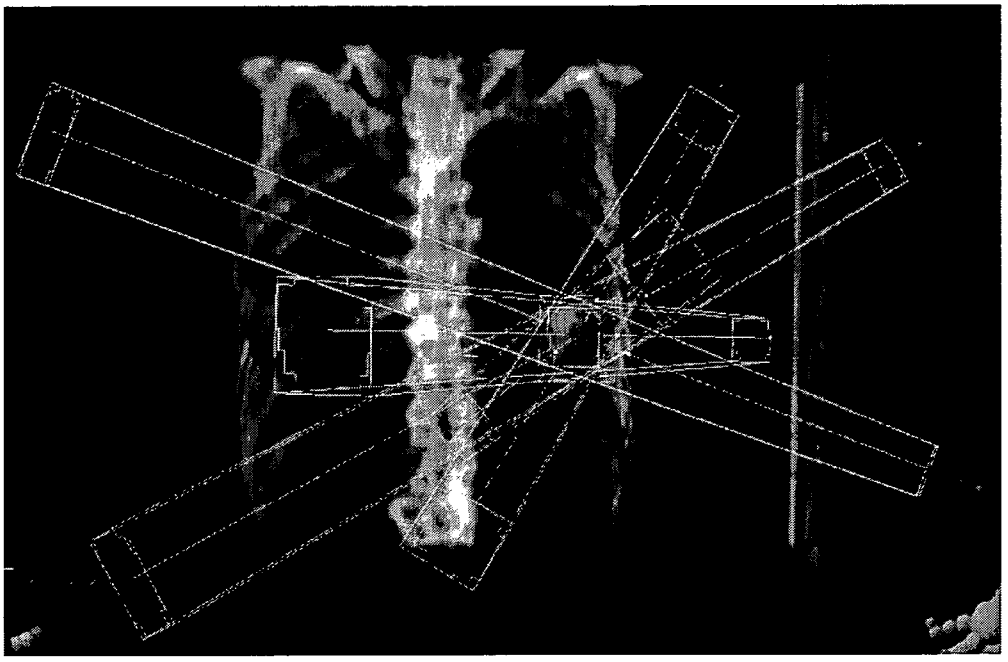

Fig. 1. Stereotactic body radiotherapy (SBRT) for lung cancer. In this image for treatment planning for left lung cancer, five beams are focused on the target

Some other fixing apparatuses using a vacuum sheet or thermoplastic shell are clinically available.

Respiratory monitoring

In the clinical practice of SBRT, the regulation of respiratory movement is essential. There are three ways to regulate the respiration of patients: respiratory holding, respiratory regulation, and respiratory gating.

The respiratory holding method is to ask patients to hold their breath for about 10s during radiation; therefore, radiation is performed intermittently four to ten times. Theoretically, this method can reduce the internal target volume (ITV). Holding can be done either voluntarily by patients or by using devices such as an active breathing control (ABC).

Respiratory regulation can be performed by exerting pressure on the abdomen using a plate like our diaphragm control or an abdominal belt.[4]

The respiratory gating method was originally developed in Japan. The gating sensors are a respiratory flow monitor, abdominal wall fiducials, and implanted gold fiducials.

Target definition

In computed tomography (CT) images taken under free-breathing long-scan (4–8s) conditions, the target outlines of the ITV are delineated. These CT images include the respiratory movement of the target. ITVs and Clinical Target Volume (CTV)s were not edited for anatomy.

If patients are irradiated with gated radiotherapy, the target outlines of CTV could be delineated under gating conditions.

The setup margins between the ITV and the planning target volume (PTV) must be determined at each institution. Our margins are 5mm for the anteroposterior (AP), 5mm for the lateral, and 8–10mm for the craniocaudal directions. Overlapping the outlines under inhale and exhale conditions is an alternative choice.

Treatment planning

There are two different concepts of Radiotherapy Treatment Planning (RTP) for SBRT. One concept, mainly used in Japan, is to maintain dose homogeneity within the target. In this case, the dose is usually prescribed at the isocenter. The other concept, mainly used in the United States, is not to maintain dose homogeneity. In this case, the dose is prescribed at the PTV margin. Our method adheres to the former concept, with selection of the optimal direction of noncoplanar beams, with the goal of the RTP being 6–10 portals for noncoplanar static beams, as shown in Fig. 1. The beam energy used was 6 MV and the isocenter was single for all beams. Four single treatments with 12Gy of radiation were prescribed at the isocenter. Using an LQ model,[5] the Biological Effective Dose (BED) was here defined to be nd (1 + d / alpha-beta) Gy, where n is the fractionation number, d is the daily dose, and the alpha-beta ratio for tumors was assumed to be 10. The value was 105.6Gy-BED for 48Gy in four fractions. The most important issue for RTP in SBRT is to maintain the dose constraints of OAR to avoid serious complications. The dose constraints of the OAR, including the spinal cord, pulmonary artery, bronchus, and heart, under the Japan Clinical Oncology Group (JCOG) 0403 protocol, are shown in Table 1.

Verification before radiation

In the clinical practice of SBRT for lung cancer, verification before each treatment is mandatory. In our institute, before each treatment, AP and lateral portal films are taken for verification. The position of each patient is verified by three experienced oncologists and technologists for each treatment. When the setup errors are larger than 2mm between the X-ray simulation film and portal film in any direction, the patient is repositioned and portal films are taken and verified again. CT on rails and FOCAL units are also useful materials for verification before each treatment.

Clinical indications for SBRT

Currently, the eligibility criteria for patients with primary lung cancer are: (1) tumor size less than 5cm in diameter without nodal and distant metastases (T14N0M0); (2) surgery was contraindicated or refused; (3) the patient could remain stable in the body frame for longer than 30min (WHO performance status <=2); (4) no active interstitial pneumonitis; and (5) written informed consent was obtained. The criteria for patients with secondary lung cancer are: (1) tumor size less than 5cm in diameter; (2) tumor number three or less; (3) no other metastases, and (4) local tumor is controlled.

Tumor size is an important factor when dose homogeneity within the target should be maintained. The dose constraints of mediastinal organs should be maintained; therefore, a central tumor could be less suitable for SBRT indications than a peripheral tumor.

Table 1. Dose constraints of various organs at risk, according to the JCOG 0403 protocol

Organ	Dose	Volume	Dose	Volume
Lung	40Gy	<=100cc	MLD	<=18cc
	V15	<=25%	V20	<=20%
Spinal cord	25Gy	Max		
Esophagus	40Gy	<=1cc	35Gy	<=10cc
Pulmonary artery	40Gy	<=1cc	35Gy	<=10cc
Stomach	36Gy	<=10cc	30Gy	<=100cc
Intestine	36Gy	<=10cc	30Gy	<=100cc
Trachea, main bronchus	40Gy	<=10cc		
Other organs (heart, etc)	48Gy	<=1cc	40Gy	<=10cc

18-Fluoro-deoxy-glucose (FDG)-positron emission tomography (PET)

18-Fluoro-deoxy-glucose (FDG)-PET scanning is an important examination both for the staging and the follow-up of lung cancer. For lung cancer staging, occult mediastinal and hilar lymph nodes, and distant metastases, are frequently found by FDG-PET.

In the follow-up of lung cancer after SBRT, radiation fibrotic change cannot be distinguished from residual tumor. FDG-PET is also useful in this situation.[6]

Clinical results

Local tumor response

The local control rates of primary lung cancer with SBRT have been previously reported by several authors, as shown in Table 2: 94 % (47/50) for 50–60Gy in five fractions with a median follow-up of 36 months,[7] 92 % (22/24) for 60Gy in 8 fractions with a median follow-up of 24 months,[8] 81% (30/37) for 60Gy in three fractions with a median follow-up of 15 months,[9] 80% for 48–60Gy in eight fractions with a median follow-up of 17 months,[10] 95% for 45–56.2Gy in three fractions with a median follow-up of 10 months,[11] 90% for 30–40Gy in four fractions with a median follow-up of 21 months,[12] and 98% (44/45) for 48Gy in four fractions with a median follow-up of 30 months.[13] However, the definition of local control after radiotherapy is difficult because local tumor failure and Radiation Induced Lung Damage (RILD) cannot be clearly delineated. Even though the definition of local control is different in various trials, a BED larger than 100Gy may be effective for the SRT of solitary lung cancer with a local control rate of above 85%.

Survival

The survival rates of stage IA (T1N0M0) lung cancer and stage IB (T2N0M0) lung cancer have not been separately reported by several authors. In our stage IA series, the 1-year and 5-year local relapse-free survival rates were 100% and 95%. The isease-free survival rates after 1, 3, and 5 years were 80%, 72%, and 72%, respectively, and the overall survival rates were 93%, 83%, and 83%, respectively. In our stage IB series, the 1-year local relapse-free survival

Table 2. Local control rates of stereotactic radiotherapy for primary lung cancer

Author (year)	Total dose (Gy)	Daily dose (Gy)	Reference point	Local control	Median follow-up (months)
Uematsu[7] (2001)	50–60	10	80% Margin	94% (47/50)	36
Arimoto[8] (1998)	60	7.5	Isocenter	92% (22/24)	24
Timmerman[9] (2003)	60	20	80% Margin	81% (30/37)	15
Onimaru[10] (2003)	48–60	6–7.5	Isocenter	80% (20/25)	17
Wulf[11] (2004)	45–56.2	15–15.4	80% Margin	95% (19/20)	10
Nagata[13] (2005)	48	12	Isocenter	98% (44/45)	30
Lee[12] (2003)	30–40	10	90% Margin	90% (8/9)	21

Table 3. Clinical toxicities after stereotactic radiotherapy for primary lung cancer

Author (year)	Number of cases	Lung >=grade 3	Lung grade 5	Other grade 5
Uematsu[7] (2001)	50	0%	0	
Arimoto[8] (1998)	24	NA	0	
Lee[12] (2003)	28	0	0%	
Onimaru[10] (2003)	45	2%	0%	Esophagus
Wulf[11] (2004)	61	0	0%	
Nagata[13] (2005)	45	0	0	
Timmerman[16] (2006)	70	20%	9%	Hemoptysis, pericarditis
J-CERG[5] (2006)	2106	NA	0.50%	Esophagus, hemoptysis

NA, not available

rate was 100%. The disease-free survivals after 1, 3, and 5-years were 92%, 71%, and 71%, respectively, and the overall survival rates were 82%, 72%, and 72%, respectively.[13] Onishi et al.[14] recently reported the results for 13 institutions in Japan, which summarized findings for 245 patients: 155 with stage IA lung cancer and 90 with stage IB lung cancer. There were 87 operable and 158 inoperable patients, and their results showed that the intercurrent death rate was especially high in the inoperable patient group. Moreover, the 5-year survival rates of operable patients irradiated with more than BED=100 Gy was 90% for stage IA and 84% for stage IB, and their clinical results were as good as those for surgery.

These survival rates should be compared with the results of surgery; however, the results of SBRT may differ depending on how many of the group are operable and how many are inoperable, and how many of the tumors are central and how many, peripheral.

Toxicities

The great concern of pulmonary toxicity with this SBRT treatment was relieved by the very low rates of complications in early studies. Most pulmonary complications were less than National Cancer Institute common toxicity criteria (NCI-CTC) version 2.0 grade 2. No other serious complications were reported, except for rib fracture, intercostals neuralgia, and mild dermatitis. However, recently, a few serious complications have been reported by several institutions in Japan.[15] These complications include grade 5 pulmonary complications, radiation pneumonitis, hemoptysis, and radiation esophagitis. Most cases of grade 5 radiation pneumonitis were associated with interstitial pneumonitis. Cases of interstitial pneumonitis should be carefully considered. Thoraco-cutaneous fistula was reported in a patient with previous tuberculosis history. Acute cholecystitis was reported in a patient with gallstones who had been pressed with an abdominal press board at the time of SBRT.

Another toxicity concern was the effect on the central bronchus, pulmonary artery, esophagus, heart, and spinal cord. The effects of a hypofractionated dose on the main bronchus, pulmonary artery, heart, and esophagus have not been followed up for a sufficiently long time. Lethal pulmonary bleeding and esophageal ulcer have been reported previously by several authors. Timmerman et al.[16] recently reported a series of complications with SBRT. Central hilar tumors adjacent to mediastinal organs should be carefully considered.[17] Table 3 shows the toxicities reported by various groups.

Ongoing clinical trials

Recently, a multi-institutional phase II study of SBRT for T1N0M0 non-small cell lung cancer under JCOG (http://www.jcog.jp/) protocol 0403 was started in Japan. Sixteen institutions entered together and started the same 48-Gy SBRT dose at the isocenter in four fractions for T1N0M0 lung cancer. One hundred patients have been registered. The results of SBRT for both inoperable and operable stage I lung cancer patients are awaited.

A new dose-escalation study of SBRT for T2N0M0 lung cancer is also planned, under the JCOG.

Timmerman et al.[9] concluded that a 60-Gy marginal dose in three fractions was the limiting dose, and the Radiation Therapy Oncology Group (RTOG) study 0239 for inoperable patients is already closed. There are a few other reports so far.[18–23] The coming RTOG protocols for operable patients, central tumors, and lung metastases are awaited.

Future directions

Both a new IGRT technique and four-dimensional RTP are future directions of SBRT. Systemic chemotherapy may be considered when the local tumor is well controlled and regional/distant metastases are frequent.

The primary indication for stereotactic radiotherapy in lung cancer could be a stage 1A (T1N0M0) patient. Very early-stage lung cancer can now be detected by screening CT examination, and these cases are also good indications for SRT; however, the issue in these cases is histological confirmation. In our clinical experience, 7 of a total of 95 SRT cases could not be finally confirmed histologically. Of course, these 7 cases were not included in our study.[13] They could not be histologically confirmed because of failure or difficulty in CT-guided biopsy or transbronchoscopic lung biopsy (TBLB). Currently, CT screening has revealed very early-stage lung cancer with ground glass opacity (GGO) and some patients with severe emphysema could be contraindicated for biopsy. Therefore, the indication for SRT for

these cases without histological confirmation should be discussed in the future. When the tumor is larger than 3 cm in diameter, which corresponds to stage 1B (T2N0M0), SRT is possible; however, the intratumor dose becomes less homogeneous, and the rate of occult distant metastases may increase. Therefore, extension of the indication of this technique for T2 tumors requires more consideration for dose escalation or adjuvant chemotherapy.

The current standard choice for stage IA lung cancer treatment is lobectomy;[24] however, for many patients this is not indicated because of accompanying diseases, such as chronic obstructive pulmonary disease (COPD), cardiac disease, and diabetes. For such patients, various minimal surgical techniques are indicated, including wedge resection and video-assisted thoracoscopic surgery (VATS), as well as ablation. The local control rates of various other modalities for primary stage I lung cancer previously reported were 93% for wedge resection and 83%-95% for VATS, and the 5-year survival rates were 82% and 50%-70%, respectively. A further randomized trial comparing SBRT with surgery should be considered.

Conclusion

SBRT is a safe and effective treatment method for stage I lung tumors. Further clinical studies are therefore warranted.

Acknowledgments This work was supported by Grant-in-aid No. 18390333, of the Ministry of Education and Science, Japan, and Grant-in-aid No. H18-014, of the Ministry of Health, Welfare, and Labor, Japan. The authors gratefully acknowledge Mr. Daniel Mrozek for his editorial assistance.

References

1. Fowler JF, Tome WA, Fenwick JD, Mehta MP (2004) A challenge to traditional radiation oncology. Int J Radiat Oncol Biol Phys 60:1241–1256
2. Blomgren H, Lax I, Goeranson H, et al. (1998) Radiosurgery for tumors in the body: clinical experience using a new method. J Radiosurg 1:63–74
3. Lax I, Blomgren H, Larson D, et al. (1998) Extracranial stereotactic radiosurgery of localized target. J Radiosurg 1:135–148
4. Negoro Y, Nagata Y, Aoki T, et al. (2001) The effectiveness of an immobilization device in conformal radiotherapy for lung tumor: reduction of respiratory tumor movement and evaluation of daily set-up accuracy. Int J Radiat Oncol Biol Phys 50:889–898
5. Yaes RJ, Patel P, Maruyama Y (1991) On using the linear-quadratic model in daily clinical practice. Int J Radiat Oncol Biol Phys 20:1353–1362
6. Ishimori T, Saga T, Nagata Y, et al. (2004) 18F-FDG and 11C-Methionine evaluation of the treatment response of lung cancer after stereotactic radiotherapy. Ann Nuclear Med 18:669–674
7. Uematsu M, Shioda A, Tahara K, et al. (2001) Computed tomography-guided frameless stereotactic radiotherapy for stage I non-small-cell lung cancer: a 5-year experience. Int J Radiat Oncol Biol Phys 51:666–670
8. Arimoto T, Usubuchi H, Matsuzawa T, et al. (1998) Small volume multiple non-coplanar arc radiotherapy for tumors of the lung, head & neck and the abdominopelvic region. In: Lemke HU (ed) CAR'98 Computer assisted radiology and surgery. Elsevier, Tokyo
9. Timmerman R, Papiez L, McGarry R et al. (2003) Extracranial stereotactic radioablation: results of a phase I study in medically inoperable stage I non-small cell lung cancer. Chest 124:1946–1955
10. Onimaru R, Shirato H, Shimizu S, et al. (2003) Tolerance of organs at risk in small-volume, hypofractionated, image-guided radiotherapy for primary and metastatic lung cancers. Int J Radiat Oncol Biol Phys 56:126–135
11. Wulf J, Haedinger U, Oppitz U, et al. (2004) Stereotactic radiotherapy for primary lung cancer and pulmonary metastases: a non-invasive treatment approach in medically inoperable patients. Int J Radiat Oncol Biol Phys 60:186–196
12. Lee S, Choi EK, Park HJ, et al. (2003) Stereotactic body frame based fractionated radiosurgery in the consecutive days for primary and metastatic tumor in the lung. Lung Cancer 40:309–315
13. Nagata Y, Negoro Y, Aoki T, et al. (2005) Clinical outcomes of a phase I/II study of 48 Gy of stereotactic body radiation therapy in four fractions using a stereotactic body frame. Int J Radiat Oncol Biol Phys 63:1427–1431
14. Onishi H, Araki T, Shirato H, et al. (2004) Stereotactic hypofractionated high-dose irradiation for stage I non-small cell lung carcinoma. Cancer 101:1623–1631
15. Nagata Y, Matsuo Y, Takayama K, et al. (2006) Survey of SBRT in Japan. Int J Radiat Oncol Biol Phys 66(Suppl. 1):s150–151
16. Timmerman R, McGarry R, Yiannoutsos C, et al. (2006) Excessive toxicity when treating central tumors in a phase II study of stereotactic body radiation therapy for medically inoperable early-stage lung cancer. JCO 24:4833–4839
17. Joyner M, Salter BJ, Papanikolaou N, Fuss M (2006) Stereotactic body radiation therapy for centrally located lung lesions. Acta Oncol 45:802–807
18. Baumann P, Nyman J, Lax I, et al. (2006) Factors important for efficacy of stereotactic body radiation therapy of medically inoperable stage I lung cancer. A retrospective analysis of patients in the Nordic countries. Acta Oncol 45:787–795
19. Liu R, Buatti JM, Howes TL, et al. (2006) Optimal number of beams for stereotactic body radiotherapy of lung and liver tumors. Int J Radiat Oncol Biol Phys 66:906–912
20. Kimura T, Matsuura K, Murakami Y, et al. (2006) CT appearance of radiation injury of the lung and clinical symptoms after stereotactic body radiation therapy (SBRT) for lung cancers: are patients with pulmonary emphysema also candidates for SBRT for lung cancers? Int J Radiat Oncol Biol Phys 66:483–491
21. Herfarth KK, Debus J, Lohr F, et al. (2000) Stereotactic single dose radiation treatment of tumors in the lung. Radiology 217(Suppl.):148
22. McGarry RC, Papiez L, Williams M, et al. (2005) Stereotactic body radiation therapy of early-stage non-small-cell lung cancer: phase I study. Int J Radiat Oncol Biol Phys 63:1010–1015
23. Beitler JJ, Badine EA, El-Savah D, et al. (2006) Stereotactic body radiation therapy for nonmetastatic lung cancer. An analysis of 75 patients over 5 years. Int J Radiat Oncol Biol Phys 65:100–106
24. Lung Cancer Study Group (1995) Randomized trial of lobectomy versus limited resection for T1N0 non-small cell lung cancer. Ann Thorac Surg 60:615–623
25. Luketich JD, Ginsberg RJ (1996) Limited resection versus lobectomy for stage I non-small cell lung cancer. In: Pass HI, Mitchell JB, Johnson DH, et al. Lung cancer: Principles and Practice. Lippincott-Raven, Philladelphia, pp 561–566

Int J Clin Oncol (2007) 12:356–362
DOI 10.1007/s10147-007-0691-9

ORIGINAL ARTICLE

**Yukinori Matsuo · Yasushi Nagata · Takashi Mizowaki
Kenji Takayama · Takashi Sakamoto · Masato Sakamoto
Yoshiki Norihisa · Masahiro Hiraoka**

Evaluation of mass-like consolidation after stereotactic body radiation therapy for lung tumors

Received: January 17, 2007 / Accepted: May 17, 2007

Abstract
Background. The purpose of this study was to evaluate the characteristics of mass-like consolidation of the lung on computed tomography (CT) after stereotactic body radiation therapy (SBRT) retrospectively.
Methods. Forty lung tumors in 37 patients who underwent SBRT were evaluated. Mass-like consolidation was defined as a dense consolidation that newly appeared over or around the original tumor, which included radiation-induced lung injury (RILI) and local recurrence. Time of appearance, initial CT findings (ectatic bronchi and conformity to dose distribution) and serial changes in the size of the mass-like consolidation were evaluated.
Results. Mass-like consolidation appeared in 27 (68%) of 40 tumors at a median of 5 months after SBRT. Follow-up examination revealed that 24 (89%) of the 27 mass-like consolidations were RILI and 3 (11%) were local recurrence. There were no significant differences in the initial CT findings between RILI and local recurrence. The size of the mass-like consolidation varied in the 12 months after SBRT. After 12 months or more, however, the size did not increase in any of the RILI cases, but it did increase in all recurrence cases.
Conclusion. Mass-like consolidations were observed in 68% of cases at a median of 5 months after SBRT. Although most of the mass-like consolidations were RILI, local recurrence was observed in a few cases. Early detection of local recurrence after SBRT was difficult.

Y. Matsuo · Y. Nagata (✉) · T. Mizowaki · K. Takayama · M. Sakamoto · Y. Norihisa · M. Hiraoka
Department of Radiation Oncology and Image-Applied Therapy, Graduate School of Medicine, Kyoto University, 54 Kawahara-cho, Shogoin, Sakyo-ku, Kyoto 606-8507, Japan
Tel./Fax +81-75-751-3418
e-mail: nag@kuhp.kyoto-u.ac.jp

T. Sakamoto
Department of Radiation Oncology, Graduate School of Medical Sciences, Kumamoto University, Kumamoto, Japan

M. Sakamoto
Department of Radiology, Japanese Red Cross Society Wakayama Medical Center, Wakayama, Japan

Key words Radiation-induced lung injury · Local recurrence · Stereotactic body radiation therapy · Lung tumor

Introduction

Stereotactic body radiation therapy (SBRT) is a newly emerging radiotherapy treatment method to deliver a high dose of radiation to the target, utilizing either a single dose or a small number of fractions with a high degree of precision within the body.[1] Compared with conventional radiation therapy, SBRT allows a high dose to be delivered to a confined area around a tumor. SBRT has been performed for lung tumors since the late 1990s. SBRT is becoming one of the principal options for the treatment of early-stage lung tumors.

After SBRT, dense consolidations are sometimes observed over or around the tumors on follow-up computed tomography (CT). Such consolidations can be confusing because they look like masses. Determining whether they represent radiation-induced lung injury (RILI) or local recurrence is difficult, though it is important from a clinical point of view. In this study, we defined a "mass-like consolidation" as a dense consolidation that newly appeared over or around the original tumor after SBRT, which included RILI and local recurrence. The purpose of this study was to evaluate the characteristics of the mass-like consolidation retrospectively.

Patients and methods

Patients

Of 52 patients who underwent SBRT for lung tumors from July 1998 through October 2002 and could be observed for more than 12 months after the completion of SBRT, 15 patients (9 who underwent chemotherapy, and 6 who had a history of previous irradiation to the thorax) were excluded. The remaining 37 patients (40 tumors) were eli-

gible for this study. Thirty patients (30 tumors) had primary lung cancer, and 7 patients (10 tumors) had metastatic lung cancer. The histological diagnoses in the 30 patients with primary lung cancer were adenocarcinoma in 17 patients, squamous cell carcinoma in 11 patients, and unknown in 2 patients. The 2 patients without histological diagnoses were clinically diagnosed as having primary lung cancer because they had no history of malignancy, their tumors had gradually grown on CT images, and diagnostic radiologists strongly suggested the tumors were primary lung cancer. The primary sites in the 7 patients with metastatic lung cancer were the colon in 2 patients (3 tumors), rectum in 2 patients (2 tumors), lung in 2 patients (3 tumors), and maxillary sinus in 1 patient (2 tumors). The median age of the patients was 77 years (range, 51–86 years). Twenty-four patients were male, and 13 were female. Follow-up duration was 13 to 65 months (median, 33 months). All patients provided written informed consent for SBRT and the associated research.

Treatment

An immobilization device (Stereotactic Body Frame; Elekta Instrument AB, Stockholm, Sweden) was used both in treatment planning and in irradiation. The planning of SBRT was performed with a commercial treatment-planning system (CADPLAN; Varian Associates, Palo Alto, CA, USA). Irradiation was performed with a 6-MV linear accelerator (CLINAC 2300C/D; Varian Associates). For the first 2 cases of primary lung cancer in this study, 40 Gy in 10-Gy fractions was prescribed at the isocenter with multiple dynamic arcs. For the other 28 cases of primary lung cancer and for 2 cases of metastatic lung cancer, 48 Gy in 12-Gy fractions was prescribed at the isocenter with multiple static ports. For the other 5 cases of metastatic lung cancer, 60 Gy in 12-Gy fractions was prescribed at the isocenter with multiple static ports. The details of the SBRT procedures were described in our previous reports.[2,3]

Follow-up CT imaging

As a rule, follow-up CT scans were performed every 3 to 6 months after SBRT. In most cases, the following scanning conditions were used: a conventional nonhelical technique at 120 kVp, 200 mAs, and a section thickness of 5 mm around the tumor and 10 mm at other sites. Nonionic iodinated contrast media were administered when the patient was not allergic to iodine and the patient consented to the use of the contrast media. Measurements of sizes of tumors and mass-like consolidations were performed under a lung window (width 900 HU and level −700 HU in most cases).

Evaluation

As described above, we defined a "mass-like consolidation" as a dense consolidation that appeared over or around the original tumor. On follow-up CT images, the maximal diameter of the original tumor treated with SBRT was measured until the tumor disappeared or was overlapped by a mass-like consolidation. When a mass-like consolidation appeared, the initial CT findings of the mass-like consolidation were evaluated, and the largest area (cm^2) of the mass-like consolidation was measured on follow-up CT images. The initial CT findings included ectatic bronchi within the mass-like consolidation and conformity to dose distribution. To evaluate the conformity of a mass-like consolidation to the dose distribution, isodose curves were superimposed on the CT images of the mass-like consolidation. When the mass-like consolidation was localized within the 16-Gy isodose curve and occupied over 60% of the area irradiated with 30 Gy or more, it was judged here to be conformal to the dose distribution.

Biopsy for confirming local recurrence could not be performed except in one patient. Therefore, the authors retrospectively evaluated which mass-like consolidations were local recurrence or RILI, based on the clinical courses of the patients, including follow-up CT images and laboratory data, and the evaluation was judged with agreement by at least two of the authors.

Statistical analysis

The Mann-Whitney *U*-test was used to compare the time of appearance between RILI and local recurrence. Fisher's exact test was used to assess differences in the rates of the initial CT findings of mass-like consolidation and to assess differences in the rate of enlargement of mass-like consolidation. Statistical significance was defined as $P < 0.05$.

Results

Seventeen of the 40 tumors reached their smallest size at a median of 8 months (range, 1–17 months) after SBRT, and 8 of these tumors finally disappeared from CT images. Twenty-three of the tumors were overlapped by mass-like consolidation, so the tumor sizes could not be evaluated thereafter. In addition to these 23 overlapping consolidations, mass-like consolidations that appeared around the original tumors and did not overlap the tumors were observed in 4 tumors. In total, mass-like consolidation was observed in 27 (68%) of the 40 tumors after SBRT.

Three of the 27 mass-like consolidations were diagnosed as local recurrences. One case, of primary squamous cell carcinoma, was histologically proven (see Fig. 1 for CT images in the patient), the second case, of metastasis from colon cancer, was diagnosed from an increase in tumor markers without other metastases, and the third case, of primary adenocarcinoma, was diagnosed from the rapid enlargement of the mass-like consolidation, associated with lymph node swelling and increasing of tumor markers (see Fig. 2 for CT images in the patient). In the remaining 24 mass-like consolidations, no evidence of local recurrence was observed (see Fig. 3 for CT findings in a representative

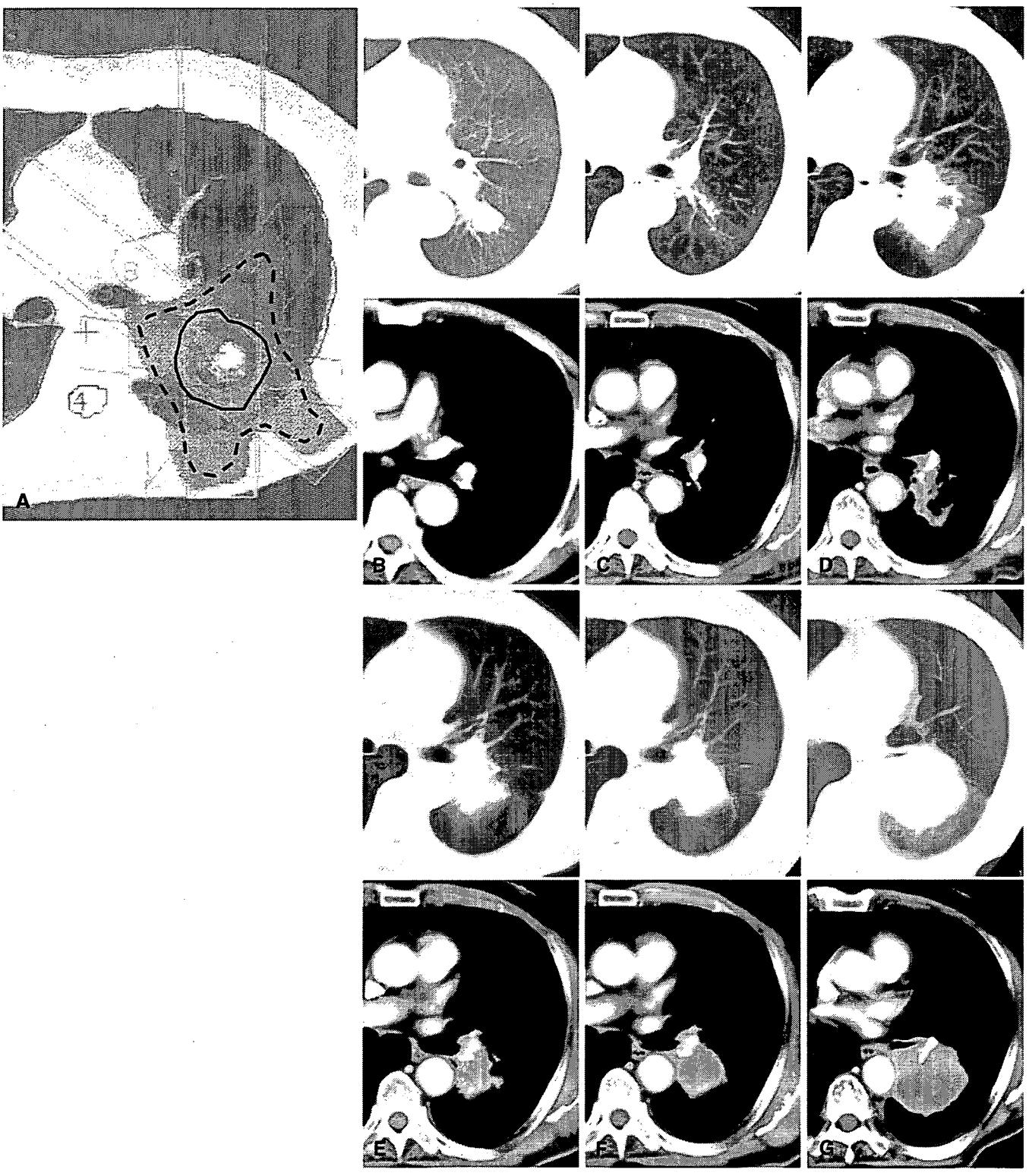

Fig. 1A–G. Serial computed tomography (CT) images in a case of local recurrence. This case, in an 81-year-old man, was a primary lung cancer that was treated with 48 Gy in 12-Gy fractions. **A** Dose distribution of treatment plan. The *inner solid line* indicates the 30-Gy isodose curve, and *the outer dashed line* indicates the 16-Gy isodose curve. **B** CT images before stereotactic body radiation therapy (SBRT) show a solitary tumor. **C** CT images 2 months after SBRT show marked shrinkage of the tumor. **D** CT images 7 months after SBRT show a mass-like consolidation. At this time, we believed this consolidation represented radiation-induced lung injury (RILI). **E** CT images 12 months after SBRT show slight shrinkage of the mass-like consolidation under the lung window. **F** CT images 16 months after SBRT show slight enlargement of the mass-like consolidation both under the lung window and under the mediastinal window. At this time, local recurrence was suspected and further examinations were recommended. However, the patient refused any examinations for the next 12 months. **G** CT images 27 months after SBRT show further enlargement of the mass-like consolidation. At this time, bronchofiberscopy was performed, and local recurrence was pathologically proven

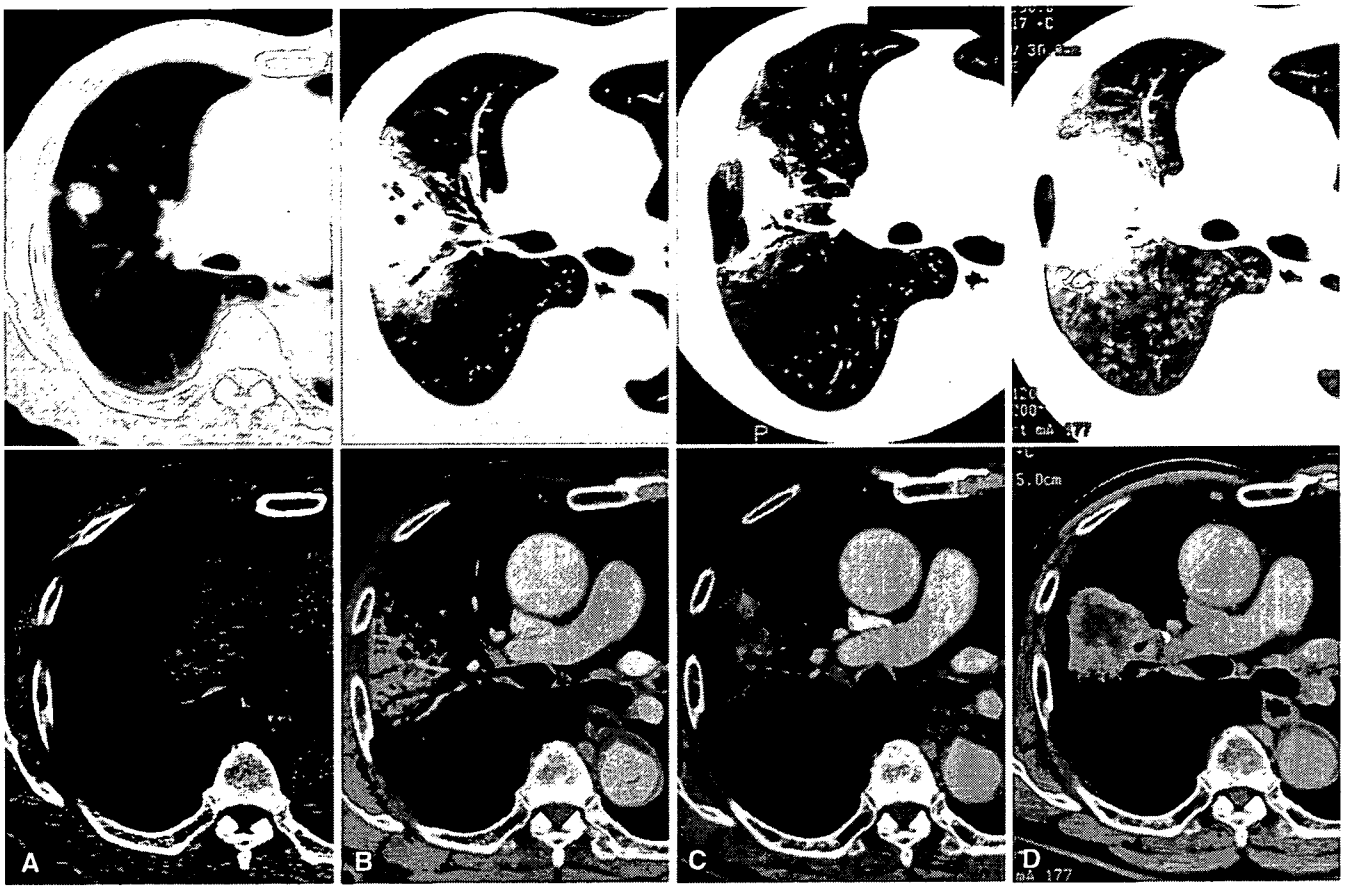

Fig. 2A–D. Serial CT images in another case of local recurrence. This case, in a 78-year-old man, was a primary lung cancer that was treated with 40 Gy in 10-Gy fractions. **A** CT images before SBRT show a solitary tumor. **B** CT images 4 months after SBRT show a mass-like consolidation with ectatic bronchi. **C** CT images 8 months after SBRT show a transient decrease in the size of the consolidation. **D** CT images 13 months after SRBT show rapid enlargement of the consolidation. At this time, lymph node swelling was observed (not shown)

case of RILI), with a median follow-up of 36 months (range, 13–65 months).

The mass-like consolidations appeared at a median of 5 months (range, 2 to 9 months) after SBRT. The time of appearance of the mass-like consolidations was 2 to 9 months (median, 5 months) in RILI cases and 4 to 7 months (median, 7 months) in local recurrence cases. There was no significant difference in the time of appearance between RILI and local recurrence ($P = 0.37$).

Ectatic bronchi within the mass-like consolidation were observed in 15 of the 24 (63%) tumors with RILI and in 1 of the 3 (33%) tumors with local recurrence. With regard to conformity to dose distribution, all mass-like consolidations were localized within 16-Gy isodose curves. The mass-like consolidations conformed to the high-dose area of 30 Gy in 11 of the 24 (46%) tumors with RILI and in 2 of the 3 (67%) tumors with local recurrence. There was no significant difference in any of these findings between RILI and local recurrence ($P = 0.55$ in ectatic bronchi, and $P = 0.60$ in conformity to dose distribution).

The size of the mass-like consolidations (Fig. 4) varied both in RILI and in local recurrence for 12 months after SBRT. Although most mass-like consolidations in RILI cases decreased in size with time, transient increases in size were observed in four mass-like consolidations. On the other hand, one mass-like consolidation in a local recurrence case temporarily decreased in size. After 12 months or more, however, the size of the mass-like consolidation did not increase in any RILI cases, but the size increased in all recurrence cases. The difference was statistically significant ($P < 0.01$).

Discussion

Clinical outcomes of SBRT for primary lung cancer have been reported by several authors, and local control rates were around 90%.[4–8] In these reports, local control was defined as "no progression of the tumors" and it was not based on the Response Evaluation Criteria in Solid Tumors (RECIST)[9] because dense consolidations sometimes overlapped the original tumors, preventing tumor sizes from being measured thereafter. In our study, 23 of the 40 tumors were overlapped by consolidations, which we defined as "mass-like consolidations."

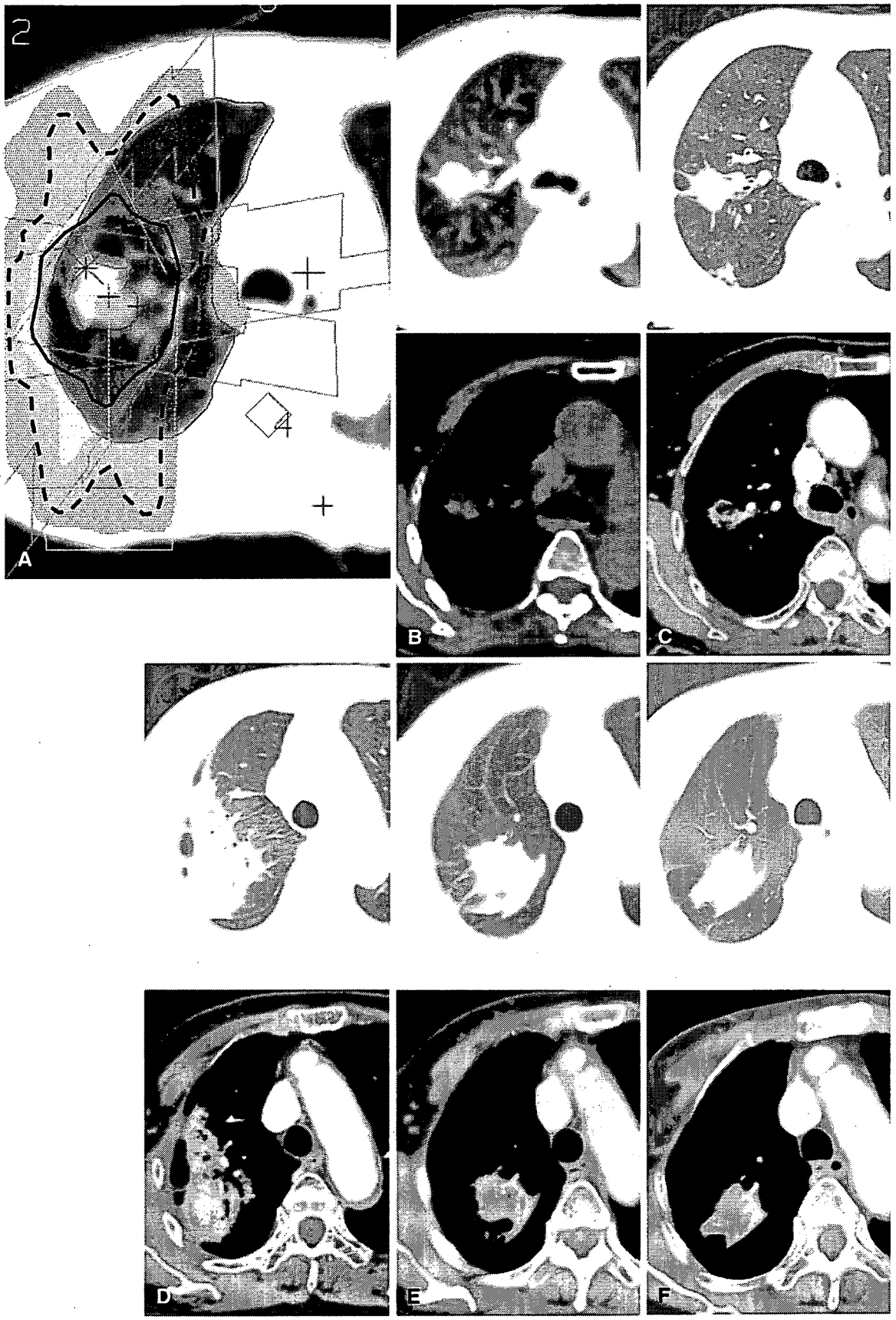

Fig. 3A–F. Serial CT images in a case of RILI. This case, in an 81-year-old woman, was a primary lung cancer that was treated with 48 Gy in 12-Gy fractions. **A** Dose distribution of treatment plan. The *inner solid line* indicates the 30-Gy isodose curve, and the *outer dashed line* indicates the 16-Gy isodose curve. **B** CT images before SBRT show a solitary tumor. **C** CT images 3 months after SBRT show no marked change. **D** CT images 6 months after SBRT show a mass-like consolidation with ectatic bronchi which overlapped the tumor. **E** CT images 16 months after SBRT show shrinkage of the consolidation. **F** CT images 56 months after SBRT show persistence of the consolidation. No evidence of local recurrence has been observed so far

For the evaluation of RILI after SBRT, dose distribution and fractionation should be considered. Compared with conventional radiotherapy, SBRT allows high doses to be delivered to a confined area around the tumor. Therefore, the dose distribution of SBRT is greatly different from that of conventional radiotherapy. Concerning fractionation, 60–66 Gy in 2-Gy fractions is commonly used in conventional radiotherapy for lung cancer. On the other hand, SBRT is performed with a much higher dose per fraction. For example, 48 Gy in 4 fractions at the isocenter is used for primary lung cancer at our institution. With respect to the correlation between the regional dose and the CT appearance of RILI, Levinson et al.[10] and Rosen et al.[11] suggested a threshold dose of 30 Gy. Using a linear-quadratic model,[12,13] with an alpha-beta ratio of 3 Gy for the evaluation of normal lung injury, 16 Gy in 4 fractions corresponds to approximately 24 Gy in 2-Gy fractions. Indeed, all of the RILI consolidations in our study appeared within the 16-Gy isodose curves.

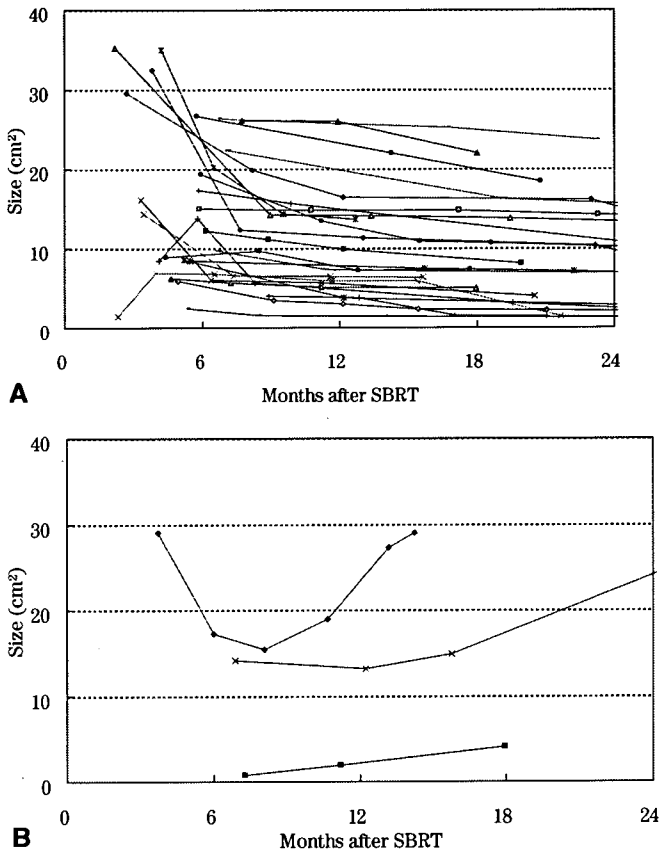

Fig. 4A,B. Serial changes in the sizes of mass-like consolidations in cases diagnosed as RILI (**A**) and cases diagnosed as local recurrence (**B**)

Several authors have reported RILI after SBRT and its classification on CT images (Table 1). Koenig et al.[14] observed modified conventional fibrosis and mass-like fibrosis in 68% cases. Aoki et al.[15] reported patchy consolidation or discrete consolidation in 74% of cases during the first 6 months after SBRT. Takeda et al.[16] reported that dense consolidation was observed in 73% of cases. Assuming that these manifestations on CT correspond to our "mass-like consolidation", our results, that mass-like consolidation appeared in 68% of tumors treated with SBRT, are in accordance with these previous results. The frequency of mass-like consolidations could be important in the evaluation of follow-up CT images after SBRT. In our study, although most of the mass-like consolidations represented RILI, a few of the mass-like consolidations turned out to represent local recurrence.

There have been a few reports on the CT differentiation of local recurrence from RILI after radiotherapy. Bourgouin et al.[17] compared CT manifestations of RILI and local recurrence after conventional radiotherapy. They suggested that RILI was consolidation with a straight lateral margin and ectatic air-containing bronchi, and that local recurrence was a soft-tissue mass with a convex lateral border and without air-containing bronchi. However, these descriptions did not always apply to our SBRT cases. Because of the differences in dose distribution described above, RILI after SBRT did not show straight lateral borders, but showed a mass-like shape. With regard to ectatic bronchi, we could not detect significant findings for the early detec-

Table 1. Summary of previous reports about radiation-induced lung injury after SBRT

	Doses	Materials	Results	Notes
Koenig et al.[14]	69.6–90.3 Gy in 33–58 fr	19 Lesions of 19 patients	Modified conventional fibrosis 26% Mass-like fibrosis 42% Scar-like fibrosis 32%	Two cases with tumor progression were excluded
Aoki et al.[15]	40–60 Gy in 4–5 fr	31 Lesions of 31 patients	≤6 Months Homogeneous pattern 26% Patchy consolidation 68% Discrete consolidation 6% >6 Months Patchy consolidation 8% Discrete consolidation 27% Solid consolidation 65%	Tumor shrank for 2–15 months after SBRT. Two cases showed tumor progression
Takeda et al.[16]	40–50 Gy in 5–8 fr	22 Lesions of 20 patients	Ground-glass opacity 33% (3–6 months) Dense consolidation 73% (3–8 months)	Dense consolidations fixed at 12 months. Four cases showed local recurrence
Present study	40 or 48 Gy in 4 fr, or 60 Gy in 5 fr	40 Lesions of 37 patients	Mass-like consolidation 68% (2–9 months)	Three cases turned out to be local recurrence

fr, fraction

tion of local recurrence. Thus, we focused attention on serial changes in the sizes of the mass-like consolidations and found a difference in enlargement 12 months or more after SBRT. Our findings were not sufficient for the early detection of local recurrence after SBRT. Further studies are required to establish a method for determining whether mass-like consolidations are RILI or local recurrence soon after SBRT.

In conclusion, mass-like consolidations were observed in 68% of cases at a median of 5 months after SBRT. Although most of the mass-like consolidations were RILI, local recurrence was observed in a few cases. Early detection of local recurrence after SBRT was difficult.

Acknowledgments This work was supported by Grants-in-Aid No. H18-014 of the Ministry of Health, Labour, and Welfare in Japan and No. 18390333 of the Japan Society for the Promotion of Science. This work was presented in part at the 90th scientific assembly and annual meeting of the RSNA in Chicago, November 28 to December 3, 2004. The authors gratefully acknowledge Mr. Daniel Mrozek for editorial assistance.

References

1. Potters L, Steinberg M, Rose C, et al. (2004) American Society for Therapeutic Radiology and Oncology and American College of Radiology practice guideline for the performance of stereotactic body radiation therapy. Int J Radiat Oncol Biol Phys 60: 1026–1032
2. Negoro Y, Nagata Y, Aoki T, et al. (2001) The effectiveness of an immobilization device in conformal radiotherapy for lung tumor: reduction of respiratory tumor movement and evaluation of the daily setup accuracy. Int J Radiat Oncol Biol Phys 50:889–898
3. Takayama K, Nagata Y, Negoro Y, et al. (2005) Treatment planning of stereotactic radiotherapy for solitary lung tumor. Int J Radiat Oncol Biol Phys 61:1565–1571
4. Uematsu M, Shioda A, Suda A, et al. (2001) Computed tomography-guided frameless stereotactic radiotherapy for stage I non-small cell lung cancer: a 5-year experience. Int J Radiat Oncol Biol Phys 51:666–670
5. Timmerman R, Papiez L, McGarry R, et al. (2003) Extracranial stereotactic radioablation: results of a phase I study in medically inoperable stage I non-small cell lung cancer. Chest 124:1946–1955
6. Onimaru R, Shirato H, Shimizu S, et al. (2003) Tolerance of organs at risk in small-volume, hypofractionated, image-guided radiotherapy for primary and metastatic lung cancers. Int J Radiat Oncol Biol Phys 56:126–135
7. Wulf J, Haedinger U, Oppitz U, et al. (2004) Stereotactic radiotherapy for primary lung cancer and pulmonary metastases: a non-invasive treatment approach in medically inoperable patients. Int J Radiat Oncol Biol Phys 60:186–196
8. Nagata Y, Takayama K, Matsuo Y, et al. (2005) Clinical outcomes of a phase I/II study of 48 Gy of stereotactic body radiotherapy in four fractions for primary lung cancer using a stereotactic body frame. Int J Radiat Oncol Biol Phys 63:1427–1431
9. Therasse P, Arbuck SG, Eisenhauer EA, et al. (2000) New guidelines to evaluate the response to treatment in solid tumors. European Organization for Research and Treatment of Cancer, National Cancer Institute of the United States, National Cancer Institute of Canada. J Natl Cancer Inst 92:205–216
10. Levinson B, Marks LB, Munley MT, et al. (1998) Regional dose response to pulmonary irradiation using a manual method. Radiother Oncol 48:53–60
11. Rosen II, Fischer TA, Antolak JA, et al. (2001) Correlation between lung fibrosis and radiation therapy dose after concurrent radiation therapy and chemotherapy for limited small cell lung cancer. Radiology 221:614–622
12. Fowler JF (1989) The linear-quadratic formula and progress in fractionated radiotherapy. Br J Radiol 62:679–694
13. Fowler JF, Tome WA, Fenwick JD, et al. (2004) A challenge to traditional radiation oncology. Int J Radiat Oncol Biol Phys 60:1241–1256
14. Koenig TR, Munden RF, Erasmus JJ, et al. (2002) Radiation injury of the lung after three-dimensional conformal radiation therapy. AJR Am J Roentgenol 178:1383–1388
15. Aoki T, Nagata Y, Negoro Y, et al. (2004) Evaluation of lung injury after three-dimensional conformal stereotactic radiation therapy for solitary lung tumors: CT appearance. Radiology 230:101–108
16. Takeda T, Takeda A, Kunieda E, et al. (2004) Radiation injury after hypofractionated stereotactic radiotherapy for peripheral small lung tumors: serial changes on CT. AJR Am J Roentgenol. 182:1123–1128
17. Bourgouin P, Cousineau G, Lemire P, et al. (1987) Differentiation of radiation-induced fibrosis from recurrent pulmonary neoplasm by CT. Can Assoc Radiol J 38:23–26

IOP PUBLISHING PHYSICS IN MEDICINE AND BIOLOGY

Phys. Med. Biol. 52 (2007) 1991–2008 doi:10.1088/0031-9155/52/7/014

An integrated Monte Carlo dosimetric verification system for radiotherapy treatment planning

T Yamamoto[1,2], T Mizowaki[2], Y Miyabe[2,3], H Takegawa[1,5], Y Narita[2], S Yano[4], Y Nagata[2], T Teshima[1] and M Hiraoka[2]

[1] Department of Medical Physics & Engineering, Osaka University Graduate School of Medicine, Suita, Osaka 565-0871, Japan
[2] Department of Radiation Oncology and Image-Applied Therapy, Kyoto University Graduate School of Medicine, Sakyo, Kyoto 606-8507, Japan
[3] Department of Nuclear Engineering, Kyoto University Graduate School of Engineering, Sakyo, Kyoto 606-8501, Japan
[4] Clinical Radiology Service Division, Kyoto University Hospital, Sakyo, Kyoto 606-8507, Japan

E-mail: teshima@sahs.med.osaka-u.ac.jp

Received 11 September 2006, in final form 6 January 2007
Published 20 March 2007
Online at stacks.iop.org/PMB/52/1991

Abstract

An integrated Monte Carlo (MC) dose calculation system, MCRTV (Monte Carlo for radiotherapy treatment plan verification), has been developed for clinical treatment plan verification, especially for routine quality assurance (QA) of intensity-modulated radiotherapy (IMRT) plans. The MCRTV system consists of the EGS4/PRESTA MC codes originally written for particle transport through the accelerator, the multileaf collimator (MLC), and the patient/phantom, which run on a 28-CPU Linux cluster, and the associated software developed for the clinical implementation. MCRTV has an interface with a commercial treatment planning system (TPS) (Eclipse, Varian Medical Systems, Palo Alto, CA, USA) and reads the information needed for MC computation transferred in DICOM-RT format. The key features of MCRTV have been presented in detail in this paper. The phase-space data of our 15 MV photon beam from a Varian Clinac 2300C/D have been developed and several benchmarks have been performed under homogeneous and several inhomogeneous conditions (including water, aluminium, lung and bone media). The MC results agreed with the ionization chamber measurements to within 1% and 2% for homogeneous and inhomogeneous conditions, respectively. The MC calculation for a clinical prostate IMRT treatment plan validated the implementation of the beams and the patient/phantom configuration in MCRTV.

(Some figures in this article are in colour only in the electronic version)

[5] Present address: Department of Radiation Oncology, Osaka Medical Center for Cancer and Cardiovascular Diseases, Higashinari, Osaka 537-8511, Japan.

0031-9155/07/071991+18$30.00

1. Introduction

Radiotherapy has become increasingly conformal since the advent of three-dimensional (3D) conformal radiotherapy (CRT) and intensity-modulated radiotherapy (IMRT). Although IMRT would achieve better dose distributions conformed to the targets while sparing the surrounding normal tissues, it simultaneously increases the complexity of beam delivery. Especially for the current IMRT systems, the conventional dose calculation algorithms often fail to predict accurate dose distributions, mainly due to the inhomogeneities in the patient anatomy and several MLC specific effects, which include the leakage radiation (LoSasso *et al* 1998), the tongue-and-groove effect (van Santvoort and Heijmen 1996, Webb *et al* 1997) and beam hardening (Fix *et al* 2001a, Kim *et al* 2001). The accuracy required for dose computation is generally between 1% and 2% (ICRU 1976, 1987, AAPM TG-65 2004); however, large errors in the doses computed by conventional dose algorithms exceeding that criterion were reported (Ma *et al* 1999, 2000, Wang *et al* 2002, Francescon *et al* 2003, Yang *et al* 2005, Sakthi *et al* 2006). These errors in dose distributions may lead to underdosage of the target or overdosage of normal tissues due to the incorrect prediction of isodose coverage. Measurements have been the standard for clinical IMRT plan quality assurance (QA) to detect such errors; however, they are often performed in low dose gradient regions where the errors in the doses computed by conventional dose algorithms are expected to be small. Furthermore, the measurements themselves may have nonnegligible errors due to the limitations, such as overresponse to low-energy photons and processor-dependent optical density values for a radiographic film.

Monte Carlo (MC) simulation has been used for external beam radiotherapy dose calculation (Mackie 1990, Mohan 1997). In general, it is now well accepted that MC is the most accurate dose calculation method, since it can precisely model realistic radiation transport through the accelerator treatment head, the MLC and the in-patient anatomy. Thus, MC has been expected as a powerful tool to obtain the accurate dose distributions, and efforts have been made to implement MC in clinical treatment planning and plan verification. Hartmann Siantar *et al* (2001) have used multiple processors and several variance reduction techniques to reduce the CPU time of the EGS4-like PEREGRINE simulations. There have been several fast MC codes developed, such as VMC/xVMC (Kawrakow *et al* 1996, Fippel *et al* 1997, Fippel 1999, Kawrakow and Fippel 2000), VMC++ (Kawrakow 2001, Cygler *et al* 2004), DPM (Sempau *et al* 2000), MCV (Siebers *et al* 2000) and MCDOSE (Ma *et al* 2002). These codes employ a variety of variance reduction techniques and achieve reduced CPU time compared to ordinary EGS4 calculations. MC is becoming fast enough to be used in clinics (especially for treatment planning purposes) with the capability of accurate dose computations.

The purpose of this study was to develop an integrated MC dose calculation system called MCRTV (Monte Carlo for radiotherapy treatment plan verification) as a routine verification tool of radiotherapy treatment plans. MCRTV was originally designed to provide the dose calculation benchmark results as accurately as possible, especially for IMRT plan QA. The MCRTV system consists of the EGS4 (Nelson *et al* 1985)/PRESTA (Bielajew and Rogers 1987) MC codes originally written for particle transport through the accelerator and the patient, and the associated software developed for the clinical implementation. We have developed and commissioned the phase-space data of a 15 MV photon beam, which is the most commonly used photon energy for IMRT at Kyoto University Hospital, by comparisons with a set of measurements under several conditions. In this paper, we describe the key features of the MCRTV system and the results of dose calculation accuracy benchmarks in detail. We also present an MCRTV calculation result for a realistic clinical IMRT plan to demonstrate the feasibility of its clinical application.

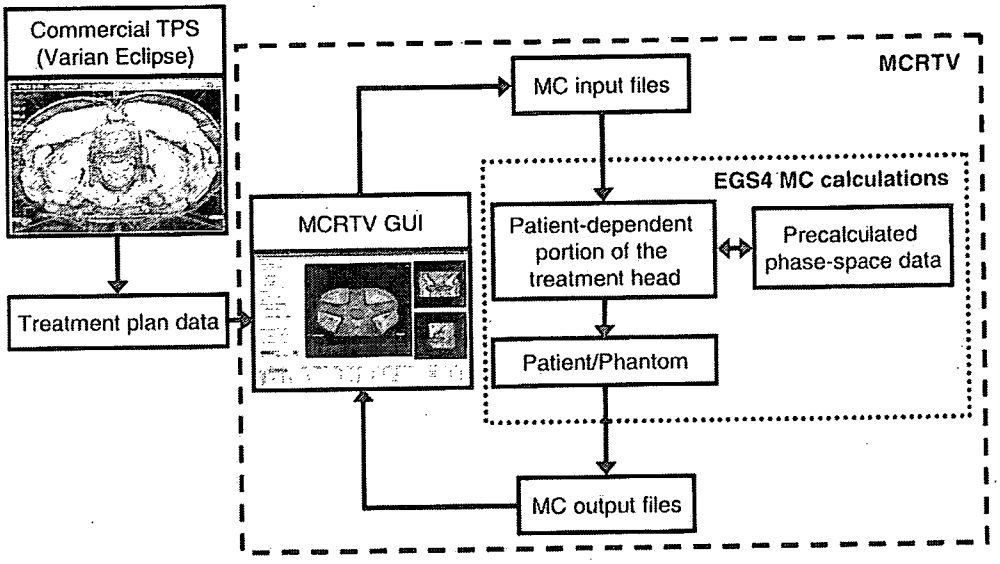

Figure 1. A schematic diagram of the MCRTV system in relationship to the Eclipse treatment planning system. The MCRTV GUI acts as an interface between MCRTV and Eclipse to read the treatment plan data, create the MC input files, and analyse the MC output dose files. The diagram indicates an ordinary flow for a given accelerator configuration; i.e., the phase-space data of the patient-independent portion of the treatment head are precalculated and used in the downstream transport calculations.

2. Methods and materials

2.1. Overview of the MCRTV system

MCRTV consists of the three MC codes, which were originally developed using EGS4/PRESTA to simulate the radiation transport through the complex geometry of the linear accelerator treatment head, the MLC and in-patient heterogeneous anatomy, which run on a 28-CPU Linux cluster, and the graphical user interface (GUI) application. MCRTV has an interface with a commercial TPS (Eclipse, Varian Medical Systems, Palo Alto, CA, USA) and reads the information needed for MC computation transferred in DICOM-RT format. With the GUI, the MC input files are created semi-automatically, the jobs are run automatically, and the output files are then processed for display and/or analysis. Figure 1 shows a schematic diagram of the MCRTV system in relationship to the Eclipse TPS. This figure represents a usual calculation flow of plan verification, in which an accelerator configuration is given and the MC calculation is performed only for the patient-related portions.

2.2. MC modelling

The MC models of the 15 MV photon beam from our Varian Clinac 2300C/D linear accelerator and the Mark II 80-leaf MLC have been developed and implemented to MCRTV as the first models. In-patient dose calculation is performed using a model built from treatment planning CT images. For the MC simulation, the treatment head is typically divided into two regions; i.e., the patient-independent and the patient-dependent portions. Thus, three MC codes were originally developed using EGS4 for the following three portions: (1) the patient-independent portion of the treatment head, (2) the patient-dependent portion of the treatment head in